

Electron-positron pair creation and correlation between momentum and energy level in a symmetric potential well

Suo Tang,¹ Bai-Song Xie,^{1,*} Ding Lu,¹ Hong-Yu Wang,² Li-Bin Fu,^{3,4} and Jie Liu^{3,4}

¹Key Laboratory of Beam Technology and Materials Modification of the Ministry of Education and College of Nuclear Science and Technology, Beijing Normal University, Beijing 100875, China

²Department of Physics, Anshan Normal University, Anshan 114005, China

³National Laboratory of Science and Technology on Computational Physics, Institute of Applied Physics and Computational Mathematics, Beijing 100088, China

⁴HEDP, Center for Applied Physics and Technology, Peking University, Beijing 100871, China

(Received 8 November 2012; published 8 July 2013)

The momentum spectrum of multiphoton-created electrons in the presence of a static potential well as well as an alternating field is found to be related to the electron energy levels in the potential well and the energy of the photons. A simple relation among three energies, the created electron energy associated with the momentum distribution, the level energy of the electron bound state, and the photon energy, is obtained. Pair production can be significantly enhanced by this two-field configuration. In this case, the depth of the static potential well and the frequency of the alternating field also need not be supercritical.

DOI: 10.1103/PhysRevA.88.012106

PACS number(s): 12.20.-m, 03.65.-w, 03.70.+k

I. INTRODUCTION

Since Sauter [1] and Schwinger [2] considered pair creation in a static electric field, vacuum electron-positron production has been studied theoretically by many authors [3–12]. In particular, using computational quantum field theory methods one can numerically solve the Dirac equation directly and investigate pair creation in much detail. There have also been several experiments on pair creation, for example, experiments at the Stanford Linac Acceleration Center (SLAC) [13] have shown that pair creation can occur in laser–electron-beam collisions. Two mechanisms are mainly responsible for pair creation in external fields. One is the Schwinger mechanism [2], which is due to a quantum tunneling effect and requires high fields $E \geq E_c = 1.32 \times 10^{16}$ V/cm. The other is due to a transition, where a high-frequency external field excites electrons with negative energy states in the Dirac sea to positive energy states, so that the photon energy plays a key role [5,14–17].

Recently, with the static Sauter potential [18] and a two-field configuration [9], new results on pair creation have been found. However, efficient pair creation with the Sauter potential requires overcritical fields that are not easy to realize. Therefore, reducing the high-field requirement becomes crucial. Motivated by this, in this paper we examine the pair creation in a symmetric potential well taking both the static Sauter potential and the alternating field into account. It is found that the width of the potential well and the frequency of the alternating field play important roles in the pair-creation process. A scaling law between the momentum spectrum of created electrons and their energy levels in the potential well is presented.

The paper is organized as follows. In Sec. II we present and discuss the relevant numerical solution of the Dirac equation. In Sec. III we obtain the relation between the momentum spectrum of the created electrons and their energy levels in

the potential well. In Sec. IV we consider the evolution of the number of particles created in the potential well under different conditions, including that of an asymmetric field. Finally, in Sec. V a summary and outline of future work are given.

II. THEORETICAL APPROACH

The evolution of the field $\hat{\psi}(z,t)$ is given by the Dirac equation [19]

$$i \frac{\partial \hat{\psi}(z,t)}{\partial t} = [c\alpha_z \hat{P} + \beta c^2 + V(z,t)] \hat{\psi}(z,t), \quad (1)$$

where $V(z,t)$ is the scalar external potential, α_z is the z component of the Dirac matrix, β is the diagonal Dirac matrix, and c is the speed of light in vacuum. Here and below the atomic units $\hbar = e = m_e = 1$ are used. We can express $\hat{\psi}(z,t)$ in terms of the electron creation and annihilation operators as

$$\begin{aligned} \hat{\psi}(z,t) &= \sum_p \hat{b}_p(t) W_p(z) + \sum_n \hat{d}_n(t) W_n(z) \\ &= \sum_p \hat{b}_p W_p(z,t) + \sum_n \hat{d}_n W_n(z,t), \end{aligned} \quad (2)$$

where $\sum_{p(n)}$ denotes summation (integration) over all states with positive (negative) energy, and $W_{p(n)}(z,t) = \langle z | p(n)(t) \rangle$ is the solution of the Dirac equation for the initial condition $W_{p(n)}(z,t=0) = W_{p(n)}(z)$, where $W_{p(n)}(z)$ is the energy eigenfunction of the field-free Dirac equation. With Eq. (2) we can express the fermion operators as

$$\hat{b}_p(t) = \sum_{p'} \hat{b}_{p'} U_{pp'}(z,t) + \sum_{n'} \hat{d}_{n'}^\dagger U_{pn'}(z,t), \quad (3)$$

$$\hat{d}_n^\dagger(t) = \sum_{p'} \hat{b}_{p'}^\dagger U_{np'}(z,t) + \sum_{n'} \hat{d}_{n'}^\dagger U_{nn'}(z,t), \quad (4)$$

$$\hat{b}_p^\dagger(t) = \sum_{p'} \hat{b}_{p'}^\dagger U_{pp'}^*(z,t) + \sum_{n'} \hat{d}_{n'} U_{pn'}^*(z,t), \quad (5)$$

$$\hat{d}_n(t) = \sum_{p'} \hat{b}_{p'}^\dagger U_{np'}^*(z,t) + \sum_{n'} \hat{d}_{n'} U_{nn'}^*(z,t), \quad (6)$$

*Corresponding author: bsxie@bnu.edu.cn

where $U_{p(n)p'(n')} = \langle p(n)|p'(n')(t)\rangle$ can be computed by first solving the Dirac wave equation starting from force-free eigenstates $|p'(n')\rangle$, and then projecting to all states $|p(n)\rangle$. The density of the created electrons is $\rho_e = \langle \text{vac}|\hat{\psi}^{(+)\dagger}(r,t)\hat{\psi}^{(+)}(r,t)|\text{vac}\rangle$, where the $\hat{\psi}^{(+)}$ is the positive-frequency part of the field operator, from which we can get the number $N(t) = \int dz \rho_e$ of created electrons. Accordingly, we have

$$\rho_e = \sum_n \left| \sum_p U_{pn}(t) W_p(z) \right|^2, \quad (7)$$

and

$$N(t) = \sum_p \langle \text{vac} | b_p^\dagger(t) b_p(t) | \text{vac} \rangle = \sum_p \sum_n |U_{pn}(t)|^2. \quad (8)$$

We then get the momentum spectrum of the created electrons

$$\rho_p = \sum_n |U_{pn}(t)|^2. \quad (9)$$

We can obtain the evolution of the states by using a split-operator technique [8,20], where the time T is discretized with N_t points and the space is limited in length L with N_z grid points. The evolution operator in each time step can be written as

$$\begin{aligned} U(t + \Delta t, t) &= \hat{T} \exp \left(-i \int_t^{t+\Delta t} [h_0 + V(z, t)] dt \right) \\ &= \exp \{ -i [h_0 + V(z, t + \Delta t/2)] \Delta t \} + O(\Delta t^3) \\ &= \exp(-iV\Delta t/2) \exp(-ih_0\Delta t) \exp(-iV\Delta t/2) \\ &\quad + O(\Delta t^3), \end{aligned} \quad (10)$$

where h_0 is the force-free Hamiltonian. Using fast Fourier transformation, we obtain the matrix elements $U_{pn}(t)$. The error in each step is of order $O(\Delta t^3)$ [8].

III. MOMENTUM SPECTRUM OF THE CREATED ELECTRONS

In our model, we have a symmetric potential well V_1 and an alternating field V_2 , so that the total field is $V(z, t) = V_1 S(z) f(t) + V_2 \sin(\omega t) S(z) \theta(t; t_0, t_0 + t_1)$, where $S(z) = \{\tanh[(z - D/2)/W] - \tanh[(z + D/2)/W]/2\}$, D is the width of the potential well, and W is a measure for the field extension at each edge. The function $f(t) = \sin[\pi t/2t_0] \theta(t; 0, t_0) + \theta(t; t_0, t_0 + t_1) + \cos[\pi(t - t_0 - t_1)/2t_0] \theta(t, t_0 + t_1, 2t_0 + t_1)$ describes the turning on and off processes of the potential well, and $\theta(t; t_1, t_2)$ is the step function. During $(0, t_0)$ the potential well exists but it is turned off at $t = t_0 + t_1$. The process for potential turning on and off can trigger pair creation [21]. In order to reduce this effect, a long duration $t_0 = 5/c^2$ is used. As soon as the potential well is well established, the oscillating field is turned on for the duration $(t_0, t_0 + t_1)$, where $t_1 = 20\pi/c^2$, i.e., several laser periods.

In Fig. 1 we present the momentum density distribution of the created electrons after the fields have been turned off. The depth of the potential well is $V_1 = 2c^2 - 10000$ and its width is $D = 10\lambda_e$, where λ_e is the Compton wavelength. The frequency of the oscillating potential is $\omega = 2.1c^2$ and its amplitude is $V_2 = 2c^2 - 10000$. As expected, the momentum

distribution is symmetrical, or $\rho(p) = \rho(-p)$. The produced electrons are accelerated by the electric field when they are created and can absorb ‘‘photons’’ in the potential well, as shown in Fig. 1(a). We have marked the value of each peak in Figs. 1(b), 1(c), 1(d), and 1(e), corresponding to the processes involving different numbers of photons.

In Fig. 1(b) we show the one-photon process. The corresponding energy of the peak number N_p can be calculated from $E^2 = p^2 + c^4$ and $p = 2\pi N_p/L$, where $L = 2.0$ is the length of the numerical grid. For example, for $N = 19$ we then obtain the electron energy $E = 1.091c^2 \simeq 1.1c^2 = \omega - c^2$. This can be considered as representing that the electron at bound-state level $-c^2$ has escaped from the Dirac sea by absorbing a photon. The energy of the peaks for $N_p = 58, 65, 72, 83, 95, 107, 118$, and 127 can be calculated easily in the same manner, leading to $E_{p1} = 1.6637c^2$, $E_{p2} = 1.7946c^2$, $E_{p3} = 1.9299c^2$, $E_{p4} = 2.1496c^2$, $E_{p5} = 2.4174c^2$, $E_{p6} = 2.6490c^2$, $E_{p7} = 2.8841c^2$, and $E_{p8} = 3.0785c^2$, respectively. On the other hand, the energy levels of the bound states in the well can be calculated from $cp_2 \cot(p_2 D) = EV_1/cp_1 - cp_1$ [22] where $p_2 = \sqrt{(E + V_1)^2/c^2 - c^2}$ and $p_1 = \sqrt{c^2 - E^2/c^2}$. We can then obtain the corresponding energy levels $E_1 = -0.4247c^2$, $E_2 = -0.3069c^2$, $E_3 = -0.1361c^2$, $E_4 = 0.0680c^2$, $E_5 = 0.2919c^2$, $E_6 = 0.5260c^2$, $E_7 = 0.7618c^2$, and $E_8 = 0.9778c^2$. From these results we can easily deduce the relation $E_{pi} = E_i + \omega$ for $i = 1$ to 8 .

The energies corresponding to the peaks with $N_p = 9, 33, 39$, and 47 are $E_{N_p=9} = 1.25c^2$, $E_{N_p=33} = 1.2539c^2$, $E_{N_p=39} = 1.3414c^2$, and $E_{N_p=47} = 1.4700c^2$, respectively. They have a somewhat more complex relation [23]. Let us turn to consider the peak $N_p = 47$. If we use the relation $E_{N_p=47} = E_0 + \omega$, we can find the corresponding peak $N_p = 150$ in Fig. 1(c) with $E_{N_p=150} = E_0 + 2\omega$ and $N_p = 242$ in Fig. 1(d) with $E_{N_p=242} = E_0 + 3\omega$, so that E_0 should be $-0.64c^2$. Instead, we find $E_0 \approx E_1 + E_2 + E_4$. We believe that these peaks may come from the high-order effects in the interaction between the energy levels and the photons [23]. Similar results are obtained for the peaks in Fig. 1(f) at $N_p = 51, 166, 267$, which we shall discuss later.

In Figs. 1(c), 1(d), and 1(e) we can also see the two-photon, three-photon, and four-photon processes, which are associated with several photons being absorbed by the created electrons. We have $E_{pn} = E_n + m\omega$, where $n = 1, 2, 3, 4, 5, 6, 7, 8$ and $m = 2, 3, 4$ for each process. It is also found that the probability of the process involving $n + 1$ photons is about one or two orders of magnitude lower than that of the n -photon process. This is consistent with the perturbation picture [9, 15, 24].

Figure 1(f) is for the same parameters as above, except that the length of the numerical grid is now $L = 2.2$ and it shows the positive momentum of the created electrons. As expected, the overall picture is similar to that in Fig. 1(a). However, the N_p values for all the peaks are 1.1 times those in Fig. 1. As an illustration, we present in the inset the values $N_{pf} = 1.1N_{pa}$ of the peaks corresponding to the two-photon process. From Figs. 1(a) and 1(f) we can see that the momentum spectrum of the created electrons does not depend on the numerical grid size.

In order ascertain that the obtained relation is independent of the system parameters, in Fig. 2 we present the numerical

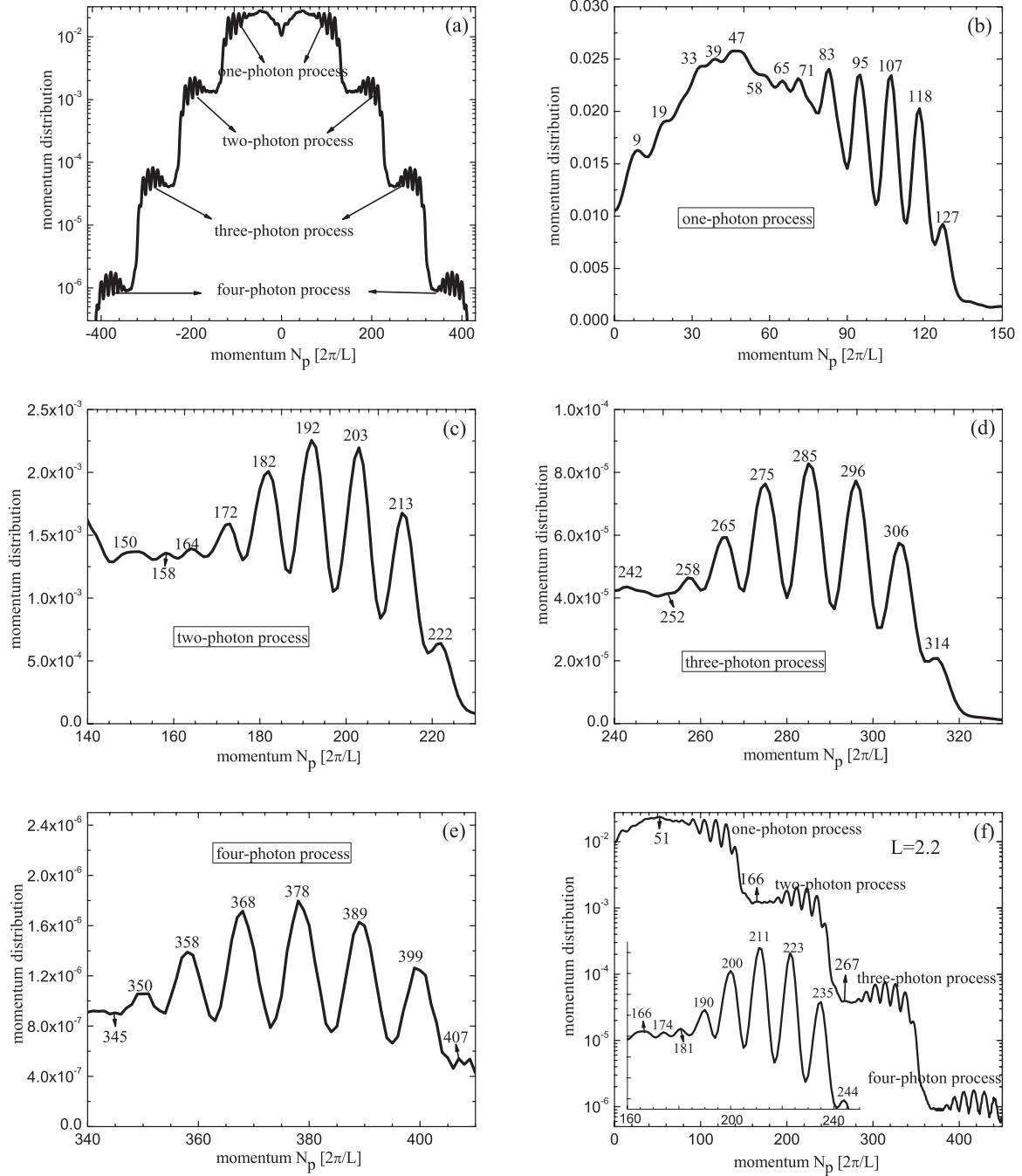


FIG. 1. Momentum spectrum of the pair-created electrons for symmetric combined fields. The frequency of the oscillating field is $\omega = 2.1c^2$. Other parameters are $N_z = 4096$, $t_0 = 5/c^2$, $t_1 = 20\pi/c^2$, $T = 2t_0 + t_1 = (10 + 20\pi)/c^2$, $N_r = 30\,000$, $D = 10\lambda_e$, $W = 0.3\lambda_e$ and $V_1 = V_2 = 2c^2 - 10\,000$. Except for (f) where the length of the numerical grid is $L = 2.2$, the other figures have the same numerical grid with $L = 2.0$.

results for $V_1 = 1.8c^2$, $V_2 = 2c^2 - 10\,000$, $D = 8.0\lambda_e$, $\omega = 1.8c^2$, and $L = 1.8$. Except for the peak $N_p = 21$ [23], we find the same relation between the energy levels and the peaks of the momentum spectrum. For simplicity, we concentrate only on the two-photon process. We find the momentum peaks at $N_{pi} = 105, 112, 123, 135, 147, 160,$ and 170 for $i = 1$ to 7 , respectively, corresponding to $E_{pi} = 2.8554c^2, 3.0231c^2, 3.2888c^2, 3.5812c^2, 3.8757c^2, 4.1965c^2,$ and $4.4443c^2$, respectively. On the other hand, the corresponding energy levels in the well are $E_i = -0.7320c^2, -0.5550c^2, -0.3129c^2,$

$-0.0358c^2, 0.2591c^2, 0.5598c^2,$ and $0.8516c^2$, respectively. That is, for $i = 1$ to 7 the simple scaling $E_{pi} = E_i + 2\omega$ applies again.

The electrons produced can also occupy the bound states in the well [25] and they can absorb one or more photons from the alternating field and then escape from the well. This multiphoton pair-creation phenomenon shows strongly the relationship between the momentum of the created electrons and the eigenenergy of the bound states. This multiphoton process also allows pair production even when the fields are subcritical.

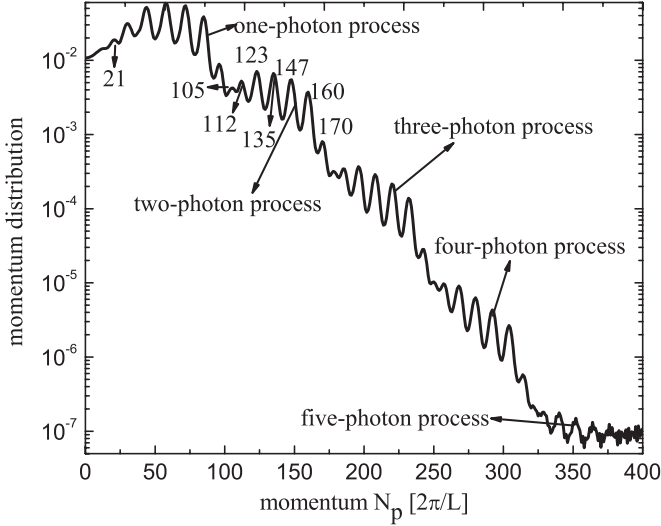


FIG. 2. Momentum spectrum of the electrons for symmetric combined fields with $\omega = 1.8c^2$, $L = 1.8$, $D = 8\lambda_e$, and $V_1 = 1.8c^2$. Other parameters are the same as in Fig. 1.

IV. EVOLUTION OF THE ELECTRON NUMBER

In this section we consider the evolution of the number of the paired electrons for different regimes. The basic parameters are $D = 10\lambda_e$, $W = 0.5\lambda_e$, and $L = 2.0$.

A. $N(t)$ at creation

Here we shall assume $V_1 = V_2 = 2c^2 - 10000$ and $\omega = 1.5c^2$ and $2.1c^2$. In Fig. 3 we present the total pair-creation electron number $N(t)$. The curve *e* in the inset corresponds to pair creation in the static potential well, i.e., $V_2 = 0$. Even though the amplitude is subcritical, we see that there are still some electrons created (because of the turning on process). The

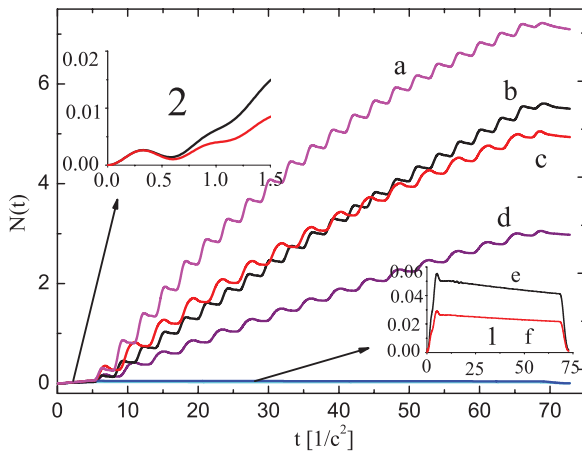


FIG. 3. (Color online) The total number $N(t)$ of the created electrons for different potentials in the cases of *a*, symmetric potential with $\omega = 2.1c^2$; *b*, asymmetric potential with $\omega = 2.1c^2$; *c* symmetric potential with $\omega = 1.5c^2$; and *d*, asymmetric potential with $\omega = 1.5c^2$. The amplitude of the static and oscillating fields is $V_1 = V_2 = 2c^2 - 10000$ except for the cases of *e*, symmetric, and *f*, asymmetric static field only, i.e., $V_2 = 0$. The other parameters are the same as in Fig. 1 except for $W = 0.5\lambda_e$.

curve *a* is for the combined field with a overcritical frequency $\omega = 2.1c^2$. We note that for the subcritical frequency $\omega = 1.5c^2$, pair creation can also be triggered, as indicated by the curve *c*.

In Fig. 3 we also show $N(t)$ for the asymmetric potential. The curve *f* is for pair creation induced by the asymmetric potential without the alternating field, and the curves *b* and *d* are for the two-field configuration, for $\omega = 2.1c^2$ and $1.5c^2$, respectively. The following can be noted. First, comparing to the two-field configuration, we see that the number of electrons created in the static-potential-alone case is negligible. The evolution of $N(t)$ exhibits oscillations at the frequency of the applied alternating field. Second, at short times the electron number in the symmetric-potential case is about twice that in the asymmetric case, which can be attributed to the two edges of the potential well. As time increases, the rate of electron creation in the symmetric potential well becomes smaller, but that in the asymmetric potential remains unchanged. This can be attributed to the suppression effect from Pauli exclusion and e^+e^- annihilation. Third, comparing the curve *b* with curve *c*, we see that even with a lower-frequency ($\omega = 1.5c^2$) alternating field, the symmetric potential well can create more electrons than the asymmetric potential with a higher-frequency ($\omega = 2.1c^2$) field. This can be attributed to the multiphoton process. If the frequency of the alternating field satisfies $\omega = E_{\text{level}} - (-c^2)$, where E_{level} is the energy of a discrete level in the potential well, pair creation can occur through quantum transitions. Thus, even when the energy of the level is low, pair creation can be realized in a combined alternating field and a static potential well.

The inset 2 in Fig. 3 shows the pair-creation process when the potential is being turned on. It is surprising that in the initial stage the symmetric and asymmetric potentials produce nearly the same number of electrons. Moreover, the particle number exhibits oscillations at a period of about $T_p \simeq 0.7/c^2$. This zeptosecond phenomenon may be associated with annihilation of the created pairs during the turning on of the external potential [26].

B. The yield $N(t)$ in the overcritical potential well

In this section we consider pair creation in an overcritical potential well with a subcritical oscillating field. We set $V_1 = 2c^2 + 10000$, $V_2 = 2c^2 - 10000$, and $\omega = 1.5c^2$. We shall again use the function $f(t)$ for the potential turn on and off.

In Fig. 4, the curve *g* describes pair creation in the static potential well. The potential well is so deep that the energy of some bound states in the well become less than $-c^2$ and they dive into the Dirac sea. As discussed in Ref. [25], the pair production rate becomes suppressed after a certain characteristic time. This suppression is associated with the complete occupation of the electron bound states with energy less than $-c^2$. However, once we add an oscillating field to the static potential well, the situation changes and the pair production process is reopened, as the curve *h* in Fig. 4 shows. Even the frequency of the oscillating field is not high enough for direct pair creation; the created electrons in the negative bound states of the potential well can absorb photons to transit to the positive states and absorb photons again to jump out of the potential well, as discussed in Sec. III.

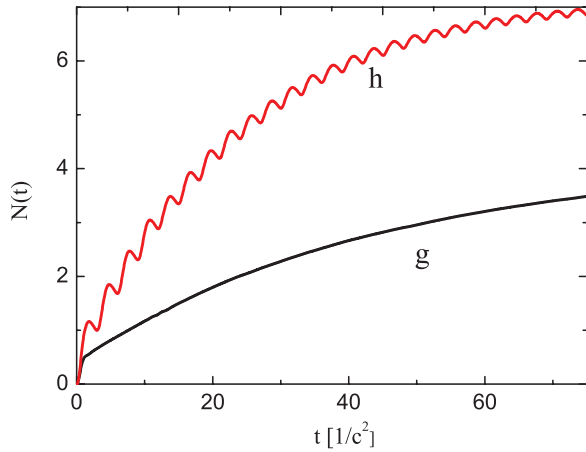


FIG. 4. (Color online) The total number of electrons created in the symmetric potential well for the cases of *g*, $V_1 = 2c^2 + 10\,000$, $V_2 = 0$, and *h*, $V_1 = 2c^2 + 10\,000$, $V_2 = 2c^2 - 10\,000$. The frequency is $\omega = 1.5c^2$. The other parameters are the same as in Fig. 1.

V. SUMMARY

We have investigated the momentum spectrum of the pair-created electrons and obtained a simple scaling law for it: $E_e = E_{\text{level}} + n\omega$. The process can be understood by noting that

electrons can stay or partly stay in the bound states when they are created. They can then escape from the well by absorbing one or more photons. One can expect that this effect also exists for potential wells with more complicated structures.

We have also discussed pair creation triggered by a combination of a subcritical potential well and an alternating field. Comparing our results from the symmetric potential well to those from the asymmetric one [9], we found that the frequency of the alternating field required for pair creation can be reduced. For long times, the growth of $N(t)$ in the symmetric potential well becomes slower, but it remains stable in the asymmetric potential. However, when an oscillating field is added to symmetrical potential, the number of created pairs always increase due to multiphoton transitions.

ACKNOWLEDGMENTS

We would like to thank Professor Ming-Young Yu for his careful reading of the manuscript and helpful improvements. This work was supported by the National Natural Science Foundation of China under Grant No. 11175023 and partially by the Open Fund of the National Laboratory of Science and Technology on Computational Physics (IAPCM). The numerical simulation was carried out at the HSCC of the Beijing Normal University.

-
- [1] F. Sauter, *Z. Phys.* **69**, 742 (1931).
 [2] J. Schwinger, *Phys. Rev.* **82**, 664 (1951).
 [3] A. I. Nikishov, *Nucl. Phys. B* **21**, 346 (1970).
 [4] A. Hansen and F. Ravndal, *Phys. Scr.* **23**, 1036 (1981).
 [5] R. Alkofer, M. B. Hecht, C. D. Roberts, S. M. Schmidt, and D. V. Vinnik, *Phys. Rev. Lett.* **87**, 193902 (2001).
 [6] F. Hebenstreit, R. Alkofer, G. V. Dunne, and H. Gies, *Phys. Rev. Lett.* **102**, 150404 (2009).
 [7] A. Nuriman, B. S. Xie, Z. L. Li, and D. Sayipjamal, *Phys. Lett. B* **717**, 465 (2012).
 [8] J. W. Braun, Q. Su, and R. Grobe, *Phys. Rev. A* **59**, 604 (1999).
 [9] M. Jiang, W. Su, Z. Q. Lv, X. Lu, Y. J. Li, R. Grobe, and Q. Su, *Phys. Rev. A* **85**, 033408 (2012).
 [10] P. Krekora, Q. Su, and R. Grobe, *Phys. Rev. Lett.* **93**, 043004 (2004).
 [11] P. Krekora, Q. Su, and R. Grobe, *Phys. Rev. Lett.* **92**, 040406 (2004).
 [12] P. Krekora, Q. Su, and R. Grobe, *Phys. Rev. A* **72**, 064103 (2005).
 [13] D. L. Burke *et al.*, *Phys. Rev. Lett.* **79**, 1626 (1997).
 [14] R. Schützhold, H. Gies, and G. Dunne, *Phys. Rev. Lett.* **101**, 130404 (2008).
 [15] W. Greiner and J. Reinhardt, *Quantum Electrodynamics*, 4th ed. (Springer-Verlag, Berlin, 2009).
 [16] W. Greiner, B. Müller, and J. Rafelski, *Quantum Electrodynamics of Strong Fields* (Springer-Verlag, Berlin, 1985).
 [17] T. Cheng, Q. Su, and R. Grobe, *Phys. Rev. A* **80**, 013410 (2009).
 [18] P. Krekora, K. Cooley, Q. Su, and R. Grobe, *Laser Phys.* **15**, 282 (2005).
 [19] S. S. Schweber, *An Introduction to Relativistic Quantum Field Theory* (Harper & Row, New York, 1962).
 [20] G. R. Mocken and C. H. Keitel, *J. Comput. Phys.* **199**, 558 (2004).
 [21] C. C. Gerry, Q. Su, and R. Grobe, *Phys. Rev. A* **74**, 044103 (2006).
 [22] W. Greiner, *Relativistic Quantum Mechanics: Wave Equations*, 3rd ed. (Springer-Verlag, Berlin, 2000).
 [23] We believe that these peaks come from the higher-order effects in the interaction between the energy levels and the photons since $E_{N_p=9} = E_3 + E_4 + \omega - c^2$, $E_{N_p=33} = E_1 + E_2 + E_3 + \omega$, $E_{N_p=39} = E_1 + E_2 + \omega$, and $E_{N_p=47} = E_1 + E_2 + E_4 + \omega$. For Fig. 2, $E_{N_p=21} = E_2 + E_3 + E_4 + E_5 + \omega$.
 [24] K. Krajewska and J. Z. Kamiński, *Phys. Rev. A* **84**, 033416 (2011).
 [25] P. Krekora, K. Cooley, Q. Su, and R. Grobe, *Phys. Rev. Lett.* **95**, 070403 (2005).
 [26] Q. Su and R. Grobe, *Laser Phys.* **17**, 92 (2007).